Electrochimica Acta 96 (2013) 274–284

Contents lists available at SciVerse ScienceDirect

Electrochimica Acta

journal homepage: www.elsevier.com/locate/electacta

Comparison of the electrochemical properties of thin films of MWCNTs/C_{60}-Pd, SWCNTs/C_{60}-Pd and ox-CNOs/C_{60}-Pd

Emilia Grądzka [a,*], Krzysztof Winkler [a], Marta Borowska [a], Marta E. Plonska-Brzezinska [a], Luis Echegoyen [b]

[a] Institute of Chemistry, University of Bialystok, Hurtowa 1, 15-399 Bialystok, Poland
[b] Department of Chemistry, University of Texas at El Paso, 500 W. University Ave., El Paso, TX 79968, USA

ARTICLE INFO

Article history:
Received 12 November 2012
Received in revised form 22 January 2013
Accepted 10 February 2013
Available online 16 February 2013

Keywords:
Electrochemical capacitors
Composites
Fullerene polymers
Carbon nanotubes
Carbon nanoonions

ABSTRACT

This work describes the study of the electrochemical properties of fullerene polymer composites, C_{60}-Pd, and different carbon nanostructures, such as single walled carbon nanotubes, multi walled carbon nanotubes and carbon nanoonions, as potential electrode materials for supercapacitors. The carbon nanostructures were deposited onto a bare gold disc electrode by a vapor deposition process. In the next step, the fullerene was electrochemically polymerized under cyclic voltammetric conditions. The obtained composites are electrochemically active at negative potentials due to the reduction of the fullerene moieties. The voltammetric response corresponding to this electrochemical process depends on the type of nanostructure and the amount of material deposited at the electrode surface. Such systems exhibit promising electrochemical properties. The highest capacitance of about 1000 F g^{-1}, with respect to mass of polymer, was obtained for the SWCNTs/C_{60}-Pd composite. This value is about four times higher compared to the capacitance of the polymer deposited on a bare gold electrode surface. Lower values of the specific capacitance were obtained for composites containing other MWCNTs and ox-CNOs. For the C_{60}-Pd/ox-CNOs composites the highest values of the specific capacitance were found to be about 280 F g^{-1}.

1. Introduction

Carbon materials, such as activated carbon [1], aerogels [2], phenolic resins [3], templated carbons [4], carbon fibers [5], and carbide derived carbons [6] have attracted a lot of attention for use as charge storage materials in high-power devices. These materials exhibit large specific surface areas, high pore accessibility, good thermal, mechanical and chemical stability, and low cost of production [7–9]. In power devices containing high surface area carbon electrodes, the charge accumulation mechanism is due to the formation of the double layer at the interface between the carbon material and the electrolyte. In the case of activated carbon, a specific capacitance of about 175 F g^{-1} can be reached [10].

Carbon materials can be also combined with redox-active materials such as transition metal oxides [11–14] or conducting polymers [12,15–17] to form very effective charge storage composites. In such systems, both power and energy density are significantly enhanced due to the faradaic process of redox-active materials. For example, specific capacitances as high as 771 F g^{-1} and 1250 F g^{-1} were reported for polyaniline/activated carbon [18] and MnO_2/CNT [19], respectively.

Since carbon nanotubes were discovered [20], a lot of work was dedicated to the development of materials containing the nanotubes and conducting polymers [21]. These systems also possess novel properties with superior characteristics than either of the individual components [22–27]. Carbon nanotube films with a high surface area allow electrochemical deposition or chemical polymerization of significant amounts of conducting polymers. Such structures have many practical applications in batteries [28–31], supercapacitors [16,32–36], biosensors [37,38], and field emission devices [39–41]. So far, most of attention has been focused on electrochemical capacitors based on carbon nanotubes [42–46] or composites of carbon nanotubes with conducting polymers [16,27,31–36,47–61]. It was shown that both MWCNTs and SWCNTs can effectively accumulate electrical charge and can be used for capacitor construction [35,54]. The specific capacitances of these materials range from 4 to 147 F g^{-1} [44,46,62–66].

In the last few years, there has been great interest in carbon nanoonions (CNOs), which constitutes an entirely new class of carbon. Carbon nanoonions, also known as spherical graphite, are built of concentric fullerene cages separated by the same distance as the shells of graphite [67]. So far little attention has been focused on the electrochemical properties of such carbon materials. It was

* Corresponding author. Tel.: +48 85 745 7827.
E-mail address: emilia@uwb.edu.pl (E. Grądzka).

0013-4686/$ – see front matter © 2013 Elsevier Ltd. All rights reserved.
http://dx.doi.org/10.1016/j.electacta.2013.02.035

found that thin films formed from unmodified carbon nanoonions are mechanically unstable. Modification of their surface with carboxylic groups allows the preparation of mechanically stable films on electrode surfaces. Similar to carbon nanotubes films, such systems exhibit typical double-layer capacitance behavior under voltammetric conditions. The specific capacitance obtained for these film in water solutions was in the range 2.29–4.74 F g^{-1} [68].

So far, most studies have been limited to composites of carbon nanotubes and *p*-type polymers [16,27,31–36,47–49,51–61]. In this paper, the electrochemical properties of composites of C_{60}-Pd and MWCNTs, SWCNTs and CNOs are compared. Studies were mainly focused on the capacitance of these materials and their electrochemical stabilities. Recently, we were investigated novel electroactive composites based on multi walled carbon nanotubes and *n*-type fullerene C_{60}-Pd polymers [69]. Since C_{60}-Pd polymers can be reduced at negative potentials, these systems exhibit *n*-doped properties [70–73]. C_{60}-Pd polymers can be formed both by electrochemical [74,75] and chemical [76] procedures. Electroreduction carried out under potentiostatic, amperostatic or potentiodynamic conditions in solution containing fullerenes and palladium(II) complexes results in the formation of polymeric phases at the electrode surface. In this system, the C_{60} is covalently bonded to the palladium in an η^2 fashion [75,77]. Similar materials can be formed chemically by reacting C_{60} with palladium(0) complexes. Films prepared from C_{60} and palladium complexes exhibit electrochemical activity in the negative potential range due to the reduction of fullerene moieties [75]. Because of its excellent reversibility and its chemical and electrochemical stability, C_{60}-Pd polymers can be used as storage materials in capacitors [75,78,79]. Depending on the conditions of film formation, two kinds of capacitors can be formed: redox capacitors in the case when the polymer is formed from solutions with a low ratio of palladium complex to C_{60} and double-layer capacitors when the polymer is formed from solutions with a high ratio of palladium complex to C_{60}. A specific capacitance of 375 F g^{-1} was reported for a C_{60}-Pd redox capacitor in acetonitrile solution containing $CsAsF_6$ as supporting electrolyte [78]. Chemically synthesized polymers exhibit much lower capacitance in comparison to electrochemically formed materials [80]. Composites containing C_{60}-Pd polymer are also electrochemically and chemically stable and exhibit very promising capacitance performance [69,81,82].

2. Experimental

Single walled carbon nanotubes, (0.7–2.5) nm in diameter and (0.5–5) μm in length, (95% purity), were purchased from Bucky USA. Multi walled carbon nanotubes, (6–13) nm in diameter and (2.5–20) μm in length, were purchased from Aldrich Chemical Co. Carbon nanoonions were produced using a procedure reported in the literature [67]. Palladium (II) acetate, $Pd(ac)_2$, from Aldrich Chemical Co. and C_{60} from M.E.R. Corp. (Tucson, AZ, USA) were used as received. The supporting electrolyte, tetra(*n*-butyl)ammonium perchlorate, $(TBA)ClO_4$, was used as received from Aldrich Chemical Co. Acetonitrile (99.9%), toluene (anhydrous, 99.8%) and dichloromethane (99.5%) received from Aldrich Chemical Co. were used without additional purification.

Cyclic voltammetry (CV) and electrochemical impedance spectroscopy (EIS) experiments were performed on an AUTOLAB (Utrecht, The Netherlands) computerized electrochemistry system equipped with the PGSTAT 12 potentiostat and FRA response analyzer expansion cards with a three-electrode cell. The frequency range for the EIS studies was in the range 10 kHz–100 mHz. The AUTOLAB system was controlled with the GPES 4.9 software of the same manufacturer. A 1.5 mm diameter gold disk from Bioanalytical Systems, Inc. (West Lafayette, IN, USA) was used as the working electrode. Prior to the experiments, the electrode was polished with a fine Carborundum paper, and then with a 0.5-μm alumina slurry. Subsequently, the electrode was sonicated in water to remove traces of alumina from the gold surface, rinsed with water, and dried. For imaging by scanning electron microscopy, SEM, the studied films were electrochemically deposited on an Au foil of Goodfellow Metals, Ltd. (Cambridge, UK). Before use, this foil was annealed in a Bunsen flame. A silver wire immersed in an acetonitrile solution of 0.01 M $AgNO_3$ and 0.09 M $(TBA)ClO_4$ that was separated from the substrate electrode by a ceramic frit from Bioanalytical Systems Inc. served as the reference electrode. The counter electrode was a platinum tab with an area of ca. 0.5 cm^2.

Simultaneous CV and piezoelectric microgravimetry (PM) experiments were performed using the EP-21 potentiostat of Elpan (Lubawa, Poland), connected to the EQCM 5710 electrochemical quartz microbalance of the Institute of Physical Chemistry Polish Academy of Science (Warsaw, Poland), which was controlled with the EQCM 5710-S2 software. This microbalance allowed for simultaneous measurements of changes of current and resonant frequency at quartz crystal resonator (Institute of Tele- and Radiocommunication, Warsaw, Poland) during potential cycling. The area of this electrode including the two contacting radial strips was 0.24 cm^2.

The studied films were imaged by secondary electron scanning electron microscopy (SEM) with the use of the Inspect S50 scanning electron microscope from FEI Company. The accelerating voltage of the electron beam was either 20 or 25 keV and the average working distance was 10 mm. Transmission electron microscopy images were obtained by Tecnai G^2 20 X-TWIN microscope of FEI Company (Hillsboro, OR, USA) with LaB6 emitter and HAADF detector for 120/200 kV.

Films of carbon nanostructures were deposited on the electrode surface by drop coating. A suitable amount of carbon nanomaterial sonically dispersed in dichloromethane was dispensed onto the electrode surface. After solvent evaporation, the electrode remained coated with a relatively porous film of the carbon nanostructures. The dry mass of the deposited carbon nanomaterials was used in the calculation of specific capacitances of the studied films.

The C_{60}-Pd film was prepared by electroreduction of an acetonitrile:toluene (1:4, *v:v*) solution containing the fullerene and $Pd(ac)_2$ and 0.1 M $(TBA)ClO_4$ as supporting electrolyte. The potential sweep rate was 100 mV s^{-1}. The mass of the deposited C_{60}-Pd polymer film was determined using PM at EQCM.

3. Results and discussion

3.1. Formation and morphology of carbon nanostructures (SWCNTs, MWCNTs, ox-CNOs) and C_{60}-Pd composites

Fig. 1 shows the CV behavior of a gold electrode coated with different carbon nanostructures, such as SWCNTs, MWCNTs, and ox-CNOs (Fig. 1a, b and c respectively). The voltammograms of all analyzed films exhibit the typical behavior for electrochemical double-layer capacitors. For the same amount of carbon nanotubes, SWCNTs and MWCNTs, different current densities were recorded. The capacitance current depends on the nature of the carbon nanomaterials as well as on the amounts of these materials deposited on the electrode surface. The specific capacitances, C_s, were calculated using the following equation:

$$C_s = \frac{\int i_c dt}{\Delta E m} \quad (1)$$

where i_c is the capacitance current, ΔE is the potential range of the integration, and m is the mass of the material deposited on the electrode surface. The current obtained for SWCNTs is about twice

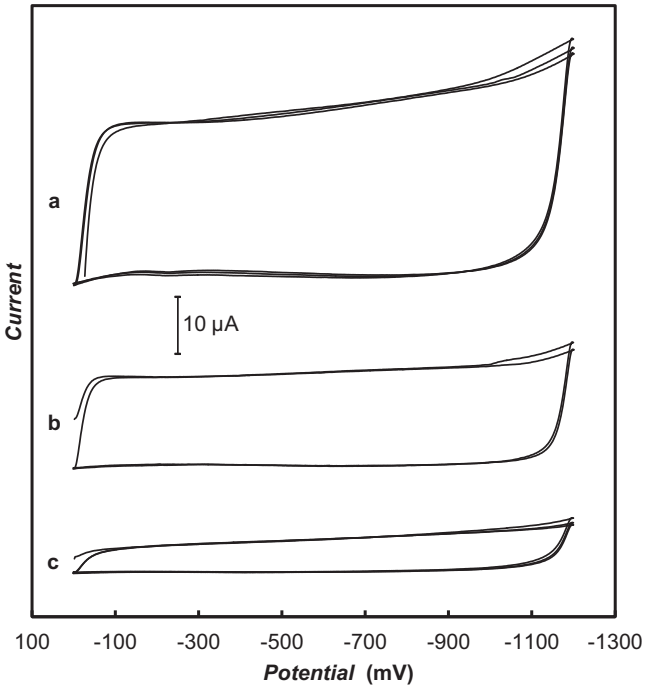

Fig. 1. Cyclic voltammograms for (a) 3.90 μg SWCNTs, (b) 3.93 μg MWCNTs and (c) 3.36 μg ox-CNOs films deposited on the 1.5 mm diameter Au disc electrode in a fresh acetonitrile solution of 0.10 M (TBA)ClO_4. The potential sweep rate was 100 mV s^{-1}.

obtained for MWCNTs. In literature, there is not agreement about capacitance performance of SWCNTs and MWCNTs [34,42,83]. In most of the reports, better capacitance properties were observed for SWCNTs [84,85]. However, it was also reported that films formed from MWCNTs exhibit higher capacitance currents than those from SWCNTs [34]. Up to date, the data reported in the literature was obtained in water. In our studies, the capacitance measurements of MWCNT and SWCNT films were also obtained in other solvents. For SWCNTs, the specific capacitance changes between 44 F g^{-1} in acetonitrile to 94 F g^{-1} in water. Much lower values of specific capacitances, in the range between 21 and 40 F g^{-1}, were obtained for MWCNTs. The best capacitance properties were observed in aqueous solutions. In the case of double layer capacitors, solvent molecules contribute to the inner layer capacitance, C_s. According to the simple mean field model for the orientation of the solvent dipoles in the field of the electrode, this contribution can be divided into two components according to the equation [86–88]:

$$\frac{1}{C_s} = \frac{4\pi d}{\varepsilon} - \frac{1}{C_{dip}} \quad (2)$$

The C_{dip} component is associated with the orientation of the solvent permanent dipoles. The distortional part, $\varepsilon/(4\pi d)$, depends on the solvent dielectric constant, ε, and the diameter, d. For aprotic solvents, the effective dipolar interactions are of the same order and the values of C_{dip} do not change significantly [89]. Therefore, the major effect of solvent on the specific capacitance of carbon nanotube films is related to the distortional component. Indeed, specific capacitances of SWCNTs and MWCNTs correlate very well with the $\varepsilon/(4\pi d)$ parameter. Linear relationships between C_s and $\varepsilon/(4\pi d)$ are observed for aprotic solvents (Fig. 2). Departures from the linear relationship for SWCNTs in water can be related to the stronger dipolar interaction (C_{dip} component).

In comparison to SWCNTs and MWCNTs, the current obtained for layers of ox-CNOs is relatively small. The specific capacitance obtained in acetonitrile containing tetra(*n*-butyl)ammonium perchlorate is 8.2 F g^{-1}. The smaller value of the specific capacitances

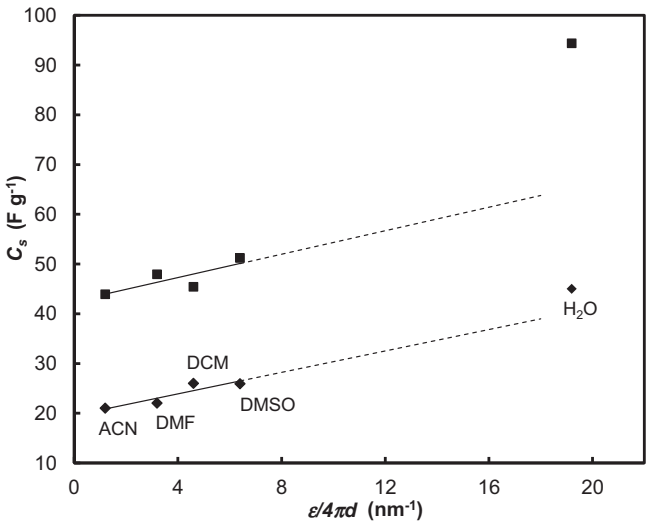

Fig. 2. Dependence of the specific capacitance with $\varepsilon/(4\pi d)$ for (■) SWCNTs and (♦) MWCNTs in different solvents. (For interpretation of the references to color in this figure legend, the reader is referred to the web version of this article.)

obtained for ox-CNOs films may be related to the more compact layer formed from this material and to the surface defects introduced upon CNO oxidation.

The C_{60}-Pd polymer was deposited on the different porous layers of carbon nanomaterials by electrochemical polymerization under CV conditions. Fig. 3 shows multicyclic CV curves of C_{60}-Pd deposition in acetonitrile/toluene (1:4, *v:v*) solution containing $Pd(ac)_2$, C_{60} fullerene, and (TBA)ClO_4 at a bare gold electrode and the gold electrode that was coated with the carbon

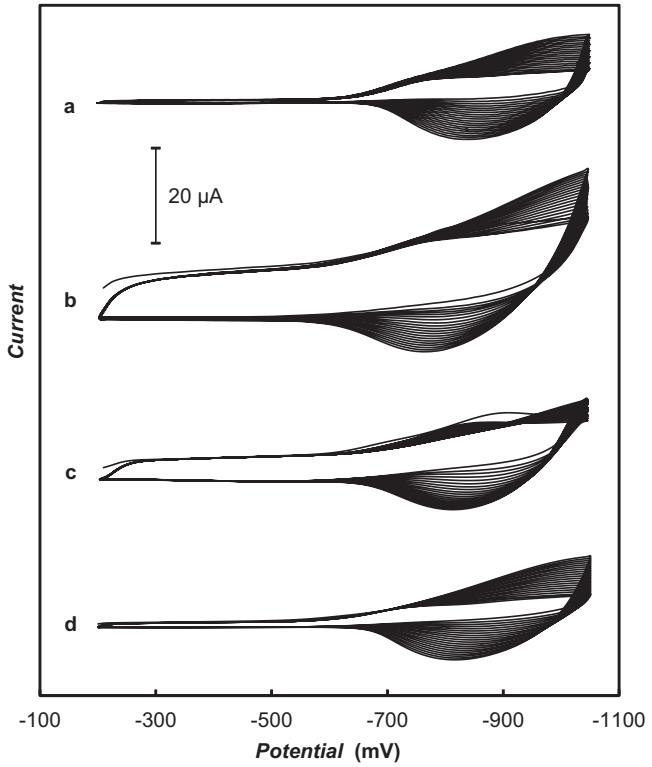

Fig. 3. Cyclic voltammograms for 0.27 mM C_{60}, 3.56 $Pd(ac)_2$ and 0.10 M (TBA)ClO_4, in acetonitrile:toluene (1:4, *v:v*) mixture recorded at (a) bare 1.5 mm diameter Au disc electrode and 1.5 mm diameter Au disc electrode coated with (b) 1.56 μg SWCNTs, (c) 1.57 μg MWCNTs and (d) 1.34 μg ox-CNOs film. The potential sweep rate was 100 mV s^{-1}.

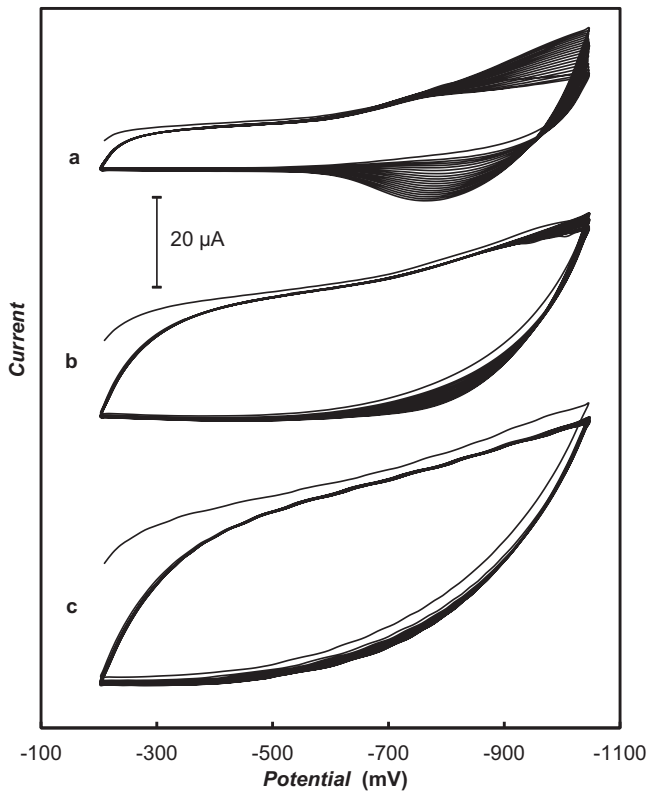

Fig. 4. Cyclic voltammograms for 0.27 mM C_{60}, 3.56 $Pd(ac)_2$ and 0.10 M $(TBA)ClO_4$, in acetonitrile:toluene (1:4, *v:v*) mixture recorded at a Au disc electrode coated with (a) 1.56 μg, (b) 3.90 μg and (c) 7.80 μg SWCNTs film. The potential sweep rate was 100 mV s^{-1}.

nanostructure films. At negative potentials, the C_{60}-Pd polymer deposition is observed. Voltammetric responses recorded during polymer deposition at a bare gold electrode (curve *a*) and electrode covered with carbon nanostructures (curves *b–d*) are similar. The process of polymer deposition depends on the thickness of the carbon nanomaterial film. Exemplary results obtained for films of SWCNTs are presented in Fig. 4. An increase of the amount of carbon material deposited at the electrode surface results in an increase of the film resistance. Therefore, for thicker films a significant decrease of the polymer deposition current is observed (Fig. 4b). Finally, for thick films (thickness higher than about 10 μm corresponding to 440 μg/cm^2) the C_{60}-Pd deposition process is completely suppressed.

The SEM images of the pristine carbon nanostructures and of the carbon nanostructures coated with the C_{60}-Pd polymer are shown in Fig. 5. During deposition of the C_{60}-Pd polymers on the carbon matrix, the fullerene polymer was attached to the carbon nanomaterials. The SWCNT layers exhibit smooth and compact structures and the C_{60}-Pd polymer formed bead shapes on the outer layers of these structures. In the case of MWCNTs/C_{60}-Pd, most of the MWCNTs is coated with homogeneous polymer layers and the nanocomposites formed a coral network. For the ox-CNOs layer, globular structures of the polymer were observed, and the carbon nanoonions are fully covered with a compact polymeric layer.

Because the surface of the SWCNTs/C_{60}-Pd and ox-CNOs/C_{60}-Pd composites was very homogeneous these systems were also examined with TEM, and some of the results are shown in Fig. 6. The TEM images clearly indicate that both nanostructures, SWCNTs and ox-CNOs, are coated with the C_{60}-Pd polymer. Carbon nanoonions form a very compact layer on the electrode surface that exhibit low porosity. In this case, the polymer is mainly deposited on top of the carbon nanoonion surface. A different morphology is observed for SWCNTs/C_{60}-Pd. The SWCNT films show high porosity compared to the ox-CNOs layer. In this system, the polymer forms spherical polymeric nanoparticles on the SWCNTs like a *pearl-necklace* with a tendency to aggregate. The diameter of these polymeric nanospeheres is relatively constant at about 85 nm.

3.2. Electrochemical properties of carbon nanostructure/C_{60}-Pd composites

The gold electrodes coated with the SWCNTs/C_{60}-Pd, MWCNTs/C_{60}-Pd and ox-CNOs/C_{60}-Pd film composites, were transferred to a fresh acetonitrile solution of the supporting electrolyte and the CV curves were recorded. The voltammograms obtained for the composites containing fullerene polymers deposited on the different carbon substrates are shown in Fig. 7. In all cases, the mass of the carbon nanomaterial deposited at the electrode surface and the mass of the electrodeposited C_{60}-Pd were the same. For comparison, the voltammogram for C_{60}-Pd electroreduction at a bare gold electrode is shown. The presence of carbon nanostructures in the composites do not drastically change the electrochemical behavior of the polymers. A charge of 3.5 and 6.8 mC/cm^2 was obtained for the C_{60}-Pd reduction for composites of MWCNTs and SWCNTs, respectively. These values are significantly higher in comparison to electreduction charge obtained for the same mass of polymer deposited at the bare electrode (2 mC/cm^2). A slightly lower value of charge corresponding to C_{60}-Pd reduction equal to 2.3 mC/cm^2 was obtained for composites containing ox-CNOs. This effect may be attributed to the different structure and porosity of these composites relative to the others (Fig. 5). The process of C_{60}-Pd reduction is accompanied by cation transport from the solution to the composite [72]. This ion doping process limits the amount of polymer that is reduced. The higher porosity of MWCNTs and SWCNTs films allows for a more effective C_{60}-Pd reduction and its doping with counter ions from solution. For all studied composites, the electrochemical behavior of C_{60}-Pd was reversible. The peak potentials for reduction and re-oxidation processes are almost the same. A small difference in these potentials were observed for MWCNTs and SWCNTs, indicating a higher resistivity of these materials.

3.3. Capacitance properties of carbon nanostructure/C_{60}-Pd composites

For potentials more positive than −0.5 V, all analyzed films exhibit the typical behavior for double-layer capacitors. In this potential range, the capacitance current is almost unaffected by the presence of the C_{60}-Pd polymer. At potentials more negative than −0.5 V, the fullerene cages are electroreduced. At these potentials, the films of the composites are quasi-rectangular in shape, which is due to the electrochemical activity of the polymeric component. A rapid response of the current with change of potential is observed. Such behavior is fundamental to ensure optimum energy storage during fast charge and discharge processes. Moreover, multiscan CV curves for these films are stable. The potential can be cyclically changed between −0.7 V and −1.2 V without a noticeable change in the shape of the voltammogram. Typical cyclic voltammograms obtained for MWCNTs/C_{60}-Pd composites for the potential range corresponding to fullerene cage electroreduction at different potential sweep rates are shown in Fig. 8a. For sweep rates lower than ca. 200 mV s^{-1}, the voltammograms show almost pseudorectangular cathodic and anodic profiles, which is characteristic for ideal capacitors. However, for higher sweep rates the CV curves deviate from an ideal rectangular shape. This effect is related to the relatively high resistance of the film of the MWCNTs/C_{60}-Pd composite and, therefore, the resulting slower current response with the potential sweep. Similar behavior was observed for the composites containing SWCNTs and ox-CNOs.

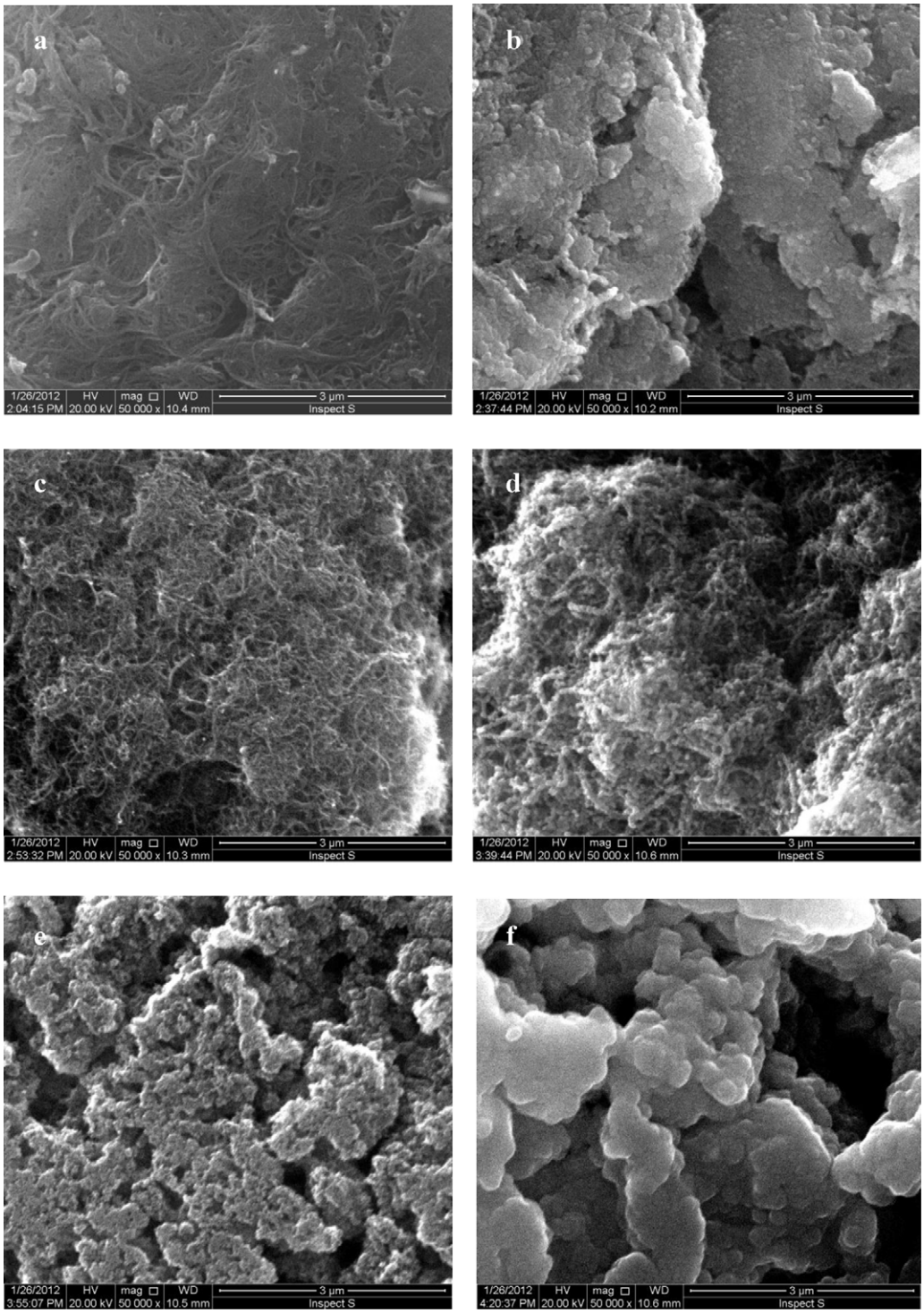

Fig. 5. SEM images of pristine (a) SWCNTs, (c) MWCNTs and (e) ox-CNOs, and of composites of (b) SWCNTs, (d) MWCNTs, (f) ox-CNOs and C_{60}-Pd polymer.

The current at negative potentials includes capacitive faradaic contributions. The magnitude of both components is predicted to depend linearly with the potential sweep rate. Therefore, a linear dependence of the total current with the potential sweep rate is expected. Such a relation between the capacitance currents and the sweep rates is shown in Fig. 8b. The specific capacitance of the composites may be calculated using the following equation:

$$C_s = \frac{i_{pc}}{Vm} \tag{3}$$

where i_{pc} is the pseudo-capacitance current and V is the potential sweep rate.

The mass of the polymer deposited at the electrode surface of the carbon nanomaterials was calculated from EQCM measurements. The carbon nanostructures dispersed in dichloromethane was dispensed onto quartz surfaces. The solvent was then evaporated and on this layer the polymer was deposited. The frequency changes of the quartz crystal during the C_{60}-Pd film deposition onto the carbon nanostructures are shown in Fig. 9. From the frequency changes, Δf, the mass of the polymeric

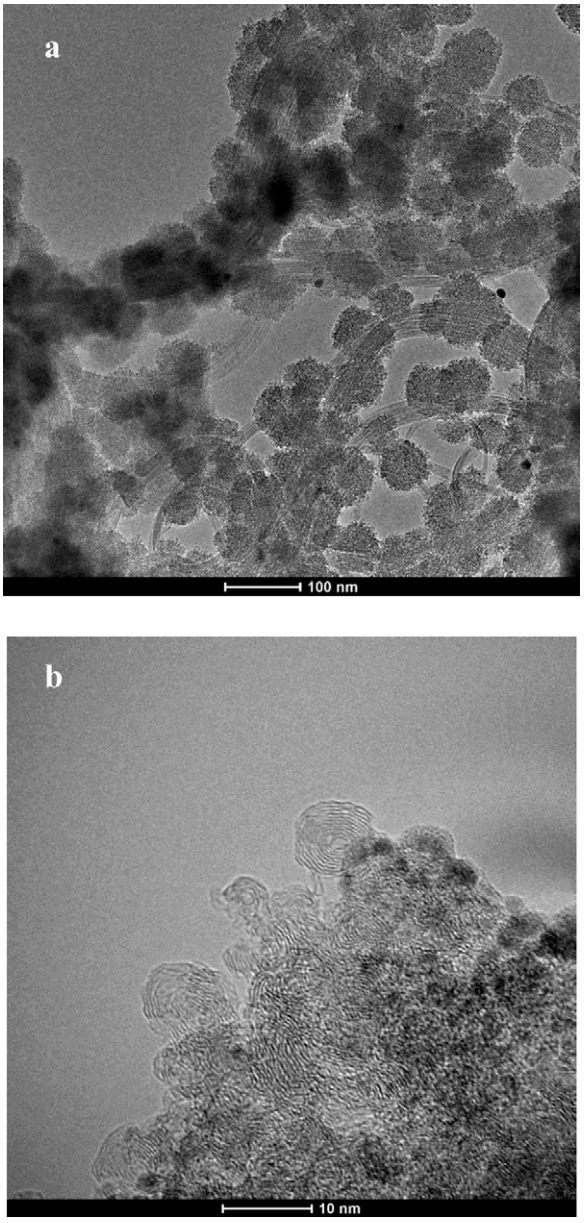

Fig. 6. TEM images of (a) SWCNTs/C_{60}-Pd and (b) ox-CNOs/C_{60}-Pd. The C_{60}-Pd polymer was deposited under CV conditions in acetonitrile:toluene (1:4, *v:v*) mixture containing 0.27 mM C_{60}, 3.56 $Pd(ac)_2$ and 0.10 M $(TBA)ClO_4$.

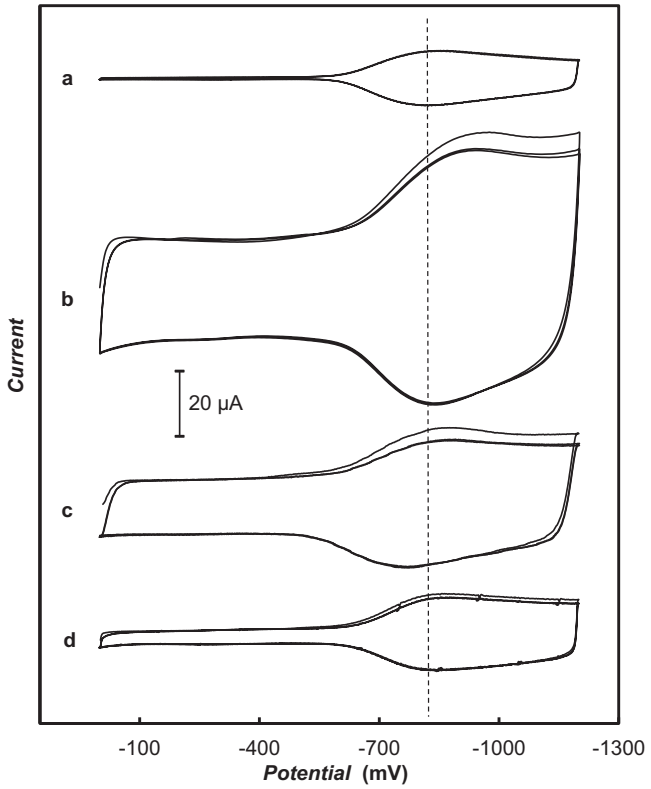

Fig. 7. Cyclic voltammograms for (a) C_{60}-Pd polymer, (b) SWCNTs/C_{60}-Pd, (c) MWCNTs/C_{60}-Pd and (d) ox-CNOs/C_{60}-Pd films in 0.10 M $(TBA)ClO_4$ in acetonitrile. The mass of the C_{60}-Pd polymer deposited at the bare gold electrode (a) was 0.531 µg. The composites containing (b) 3.90 µg SWCNTs and 0.77 µg C_{60}-Pd, (c) 3.93 µg MWCNTs and 0.68 µg C_{60}-Pd and (d) 3.36 µg ox-CNOs and 0.65 µg C_{60}-Pd. The potential sweep rate was 100 mV s^{-1}.

material was calculated using Sauerbrey equation: $\Delta m = 17.7\ \Delta f$ ng Hz^{-1} cm^{-2}.

The specific capacitance was calculated using Eq. (1) for the potential range where the polymer is conducting. This pseudo-capacitance current mainly results from electroreduction of the C_{60}-Pd polymer. The higher specific capacitance, equal to about 990 F g^{-1}, was obtained for the C_{60}-Pd polymer deposited on the SWCNTs film. In the same way the capacitance calculated for the other composites were 758 F g^{-1} and 284 F g^{-1}, for MWCNTs/C_{60}-Pd and ox-CNOs/C_{60}-Pd, respectively. The values obtained for SWCNTs/C_{60}-Pd and MWCNTs/C_{60}-Pd are several times higher when compared to the C_{60}-Pd film deposited on the surface of the bare gold electrode (C_s = 200 F g^{-1}) [78].

The effect of the composition of the carbon nanostructures/C_{60}-Pd composites on their capacitive behavior was also investigated. We studied the influence of the amount of carbon nanostructures and the amount of polymer on the capacitance of the analyzed composites. The specific capacitance values, calculated for all analyzed compositions of all layers are summarized in Table 1. Fig. 10 shows that the capacitance is stable and independent of sweep rate.

The key requirement for commercial application of materials in electronics, energy storage devices and batteries, is their electrochemical stability. Electrochemical stability of electroactive films depends on different parameters, such as the synthesis conditions and the nature of the cation doping the layer and of the solvent.

Table 1
Specific capacitance for the carbon nanostructures/C_{60}-Pd composites in 0.1 M $(TBA)ClO_4$ in acetonitrile.

Specific capacitance (F g^{-1})						
$m_{carbon\ nanostructures}/m_{C60Pd}$	Based on the composite mass			Based on the C_{60}-Pd mass		
	SWCNTs/C_{60}-Pd	MWCNTs/C_{60}-Pd	ox-CNOs/C_{60}-Pd	SWCNTs/C_{60}-Pd	MWCNTs/C_{60}-Pd	ox-CNOs/C_{60}-Pd
2	65	27	20	196	89	62
5	56	28	14	339	189	86
10	59	31	17	661	394	189
15	61	60	17	994	758	284

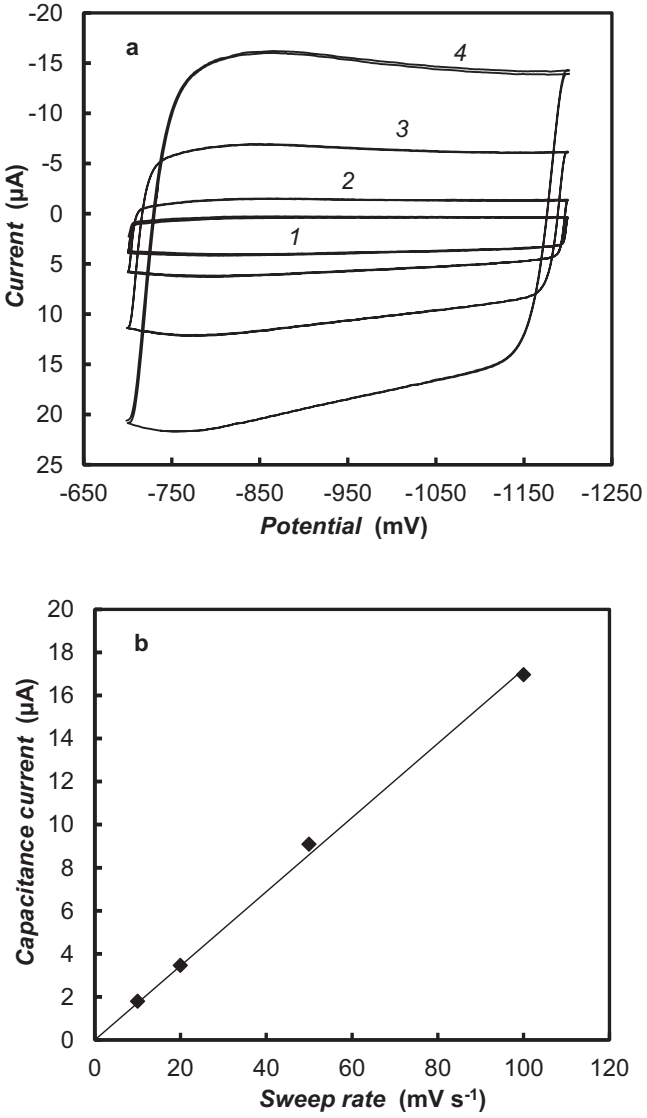

Fig. 8. (a) Cyclic voltammograms for the MWCNTs/C_{60}-Pd film containing 3.93 μg MWCNTs and 0.68 μg C_{60}-Pd in 0.10 M (TBA)ClO_4 in acetonitrile. The potential sweep rate was (*1*) 10 mV s^{-1}, (*2*) 20 mV s^{-1}, (*3*) 50 mV s^{-1}, (*4*) 100 mV s^{-1}. (b) Dependence of the current at −950 mV on the potential sweep rate for the MWCNTs/C_{60}-Pd film containing 3.93 μg MWCNTs and 0.68 μg C_{60}-Pd.

We studied the influence of the potential window on the electrochemical stability of the composites, in acetonitrile solution containing (TBA)ClO_4 as supporting electrolyte. The SWCNTs/C_{60}-Pd film is stable down to −2.7 V. At more negative potentials, a slow decomposition of the polymer is observed. Fig. 11a shows multicyclic voltammograms of the SWCNTs/C_{60}-Pd recorded within a potential range between 0 and −2.8 V. Progressive decomposition of the composite is observed for every cycle but the decomposition percent is very small. It has to be stressed that this composite is much more stable when compared to the C_{60}-Pd polymer alone [90]. Similar behavior for the MWCNTs/C_{60}-Pd composite was observed. In the case of ox-CNOs/C_{60}-Pd composite, it slowly decomposed at a potential of −1.5 V. The stable potential range of the composite based on ox-CNOs is lower to that of the C_{60}-Pd film deposited at a bare metallic electrode. In acetonitrile solution containing (TBA)ClO_4, the C_{60}-Pd polymer decomposed at −1.8 V [90]. The composites containing SWCNTs and MWCNTs are the most stable because of their excellent mechanical strength.

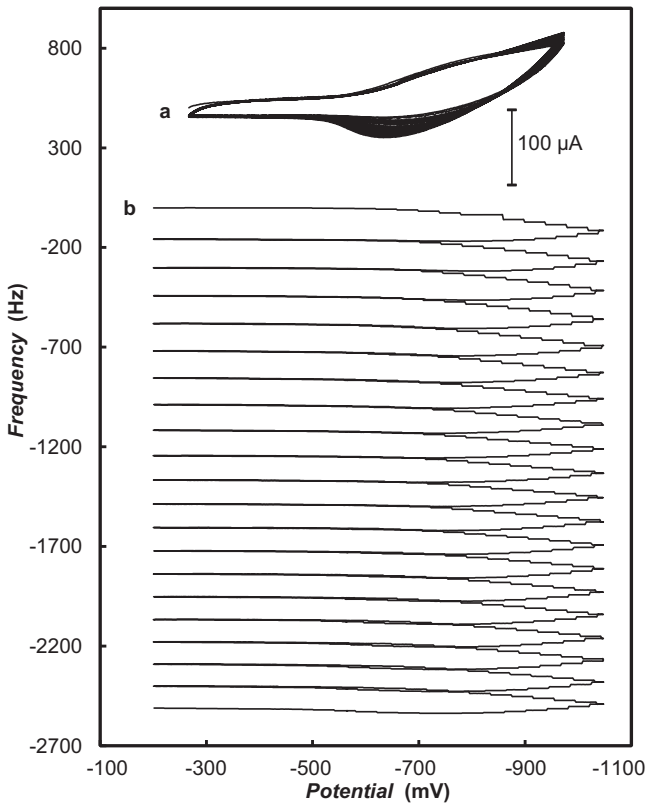

Fig. 9. (a) Cyclic voltammogram and (b) curves of the frequency change vs potential recorded at the Au/quartz electrode coated with the 3.90 μg SWCNTs in acetonitrile:toluene (1:4, *v:v*) mixture containing 0.27 mM C_{60}, 3.56 $Pd(ac)_2$ and 0.10 M (TBA)ClO_4. The potential sweep rate was 100 mV s^{-1}.

Structures containing these carbon materials are difficult to destroy completely. In all cases, even after prolonged potential scanning to very negative potentials, the film is not completely removed from the surface of the electrode. A stationary background

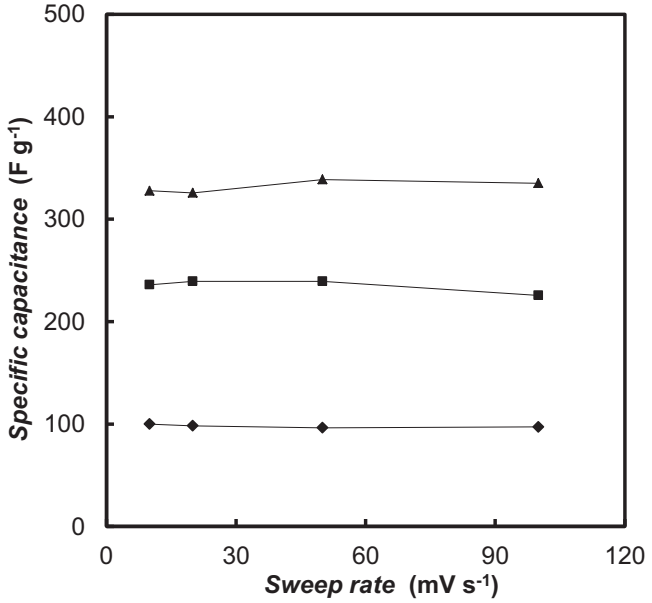

Fig. 10. Specific capacitance of (▲) SWCNTs/C_{60}-Pd, (■) MWCNTs/C_{60}-Pd and (♦) ox-CNOs/C_{60}-Pd as a function of scan rate recorded in acetonitrile containing 0.10 M (TBA)ClO_4. The composites containing (▲) 3.90 μg SWCNTs and 0.77 μg C_{60}-Pd, (■) 3.93 μg MWCNTs and 0.68 μg C_{60}-Pd and (♦) 3.36 μg ox-CNOs and 0.65 μg C_{60}-Pd.

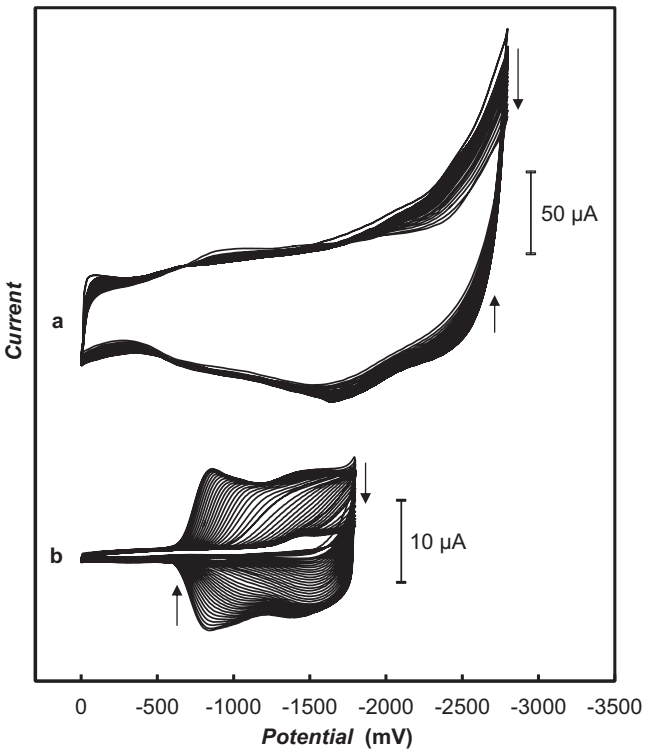

Fig. 11. Cyclic voltammograms for (a) SWCNTs/C_{60}-Pd and (b) C_{60}-Pd films in 0.10 M (TBA)ClO_4 in acetonitrile. The composite containing 3.90 μg SWCNTs and 0.77 μg C_{60}-Pd. The mass of the C_{60}-Pd polymer deposited at the bare gold electrode was 0.531 μg. The potential sweep rate was 100 mV s^{-1}.

current is observed in voltammograms recorded after prolonged potential scanning. Moreover, thin layers initially grown on the electrode surface exhibit higher stability in negative potential range. These systems are more stable than the pure C_{60}-Pd polymer (Fig. 11b).

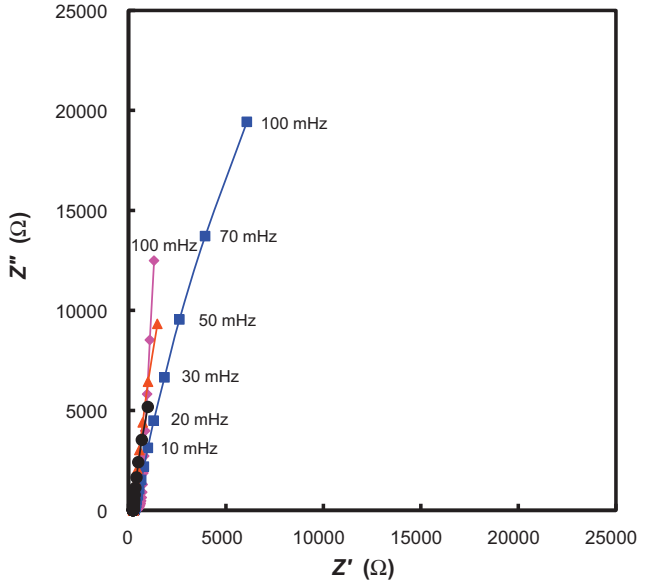

Fig. 12. Nyquist plots for (♦) C_{60}-Pd polymer, (●) SWCNTs/C_{60}-Pd, (▲) MWCNTs/C_{60}-Pd and (■) ox-CNOs/C_{60}-Pd films in acetonitrile containing 0.10 M (TBA)ClO_4 at −1200 mV. The composites containing (●) 3.90 μg SWCNTs and 0.77 μg C_{60}-Pd, (▲) 3.93 μg MWCNTs and 0.68 μg C_{60}-Pd and (■) 3.36 μg ox-CNOs and 0.65 μg C_{60}-Pd. The mass of the C_{60}-Pd polymer deposited at the bare gold electrode was 0.531 μg. The frequency range was 10 kHz -100 mHz. (For interpretation of the references to color in this figure legend, the reader is referred to the web version of this article.)

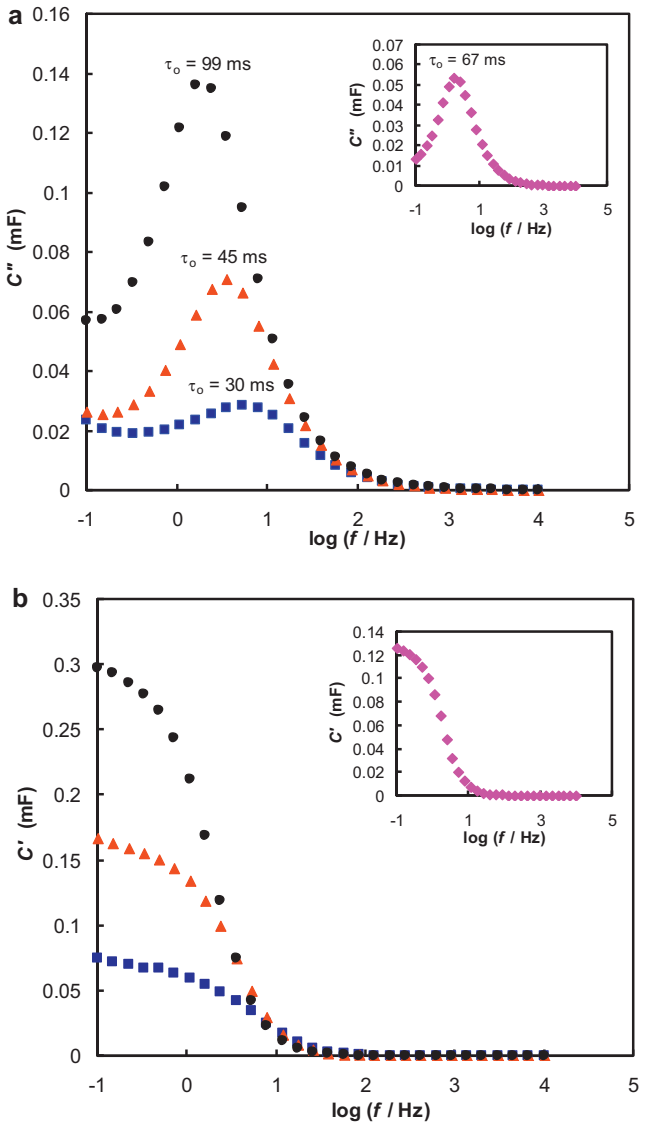

Fig. 13. (a) Dependence of the imaginary part of capacitance on frequency and (b) dependence of real part of capacitance on frequency for (♦) C_{60}-Pd polymer, (●) SWCNTs/C_{60}-Pd, (▲) MWCNTs/C_{60}-Pd and (■) ox-CNOs/C_{60}-Pd films in acetonitrile containing 0.10 M (TBA)ClO_4 at -1200 mV. The composites containing (●) 3.90 μg SWCNTs and 0.77 μg C_{60}-Pd, (▲) 3.93 μg MWCNTs and 0.68 μg C_{60}-Pd and (■) 3.36 μg ox-CNOs and 0.65 μg C_{60}-Pd. The mass of the C_{60}-Pd polymer deposited at the bare gold electrode was 0.531 μg. (For interpretation of the references to color in this figure legend, the reader is referred to the web version of this article.)

The composites were also investigated by electrochemical impedance spectroscopy. The Nyquist plots of the composites at potentials at which the fullerene cages are reduced exhibit a vertical trend at low frequencies (Fig. 12), indicating capacitive behavior. In the case of plots obtained for the ox-CNOs/C_{60}-Pd composite, the capacitive behavior was replaced by a more inclined diffusion line. Since the charge transfer step is very fast and the capacitance of the system very high, the semicircle feature related to the charge transfer process is not observed on Z''–Z' graphs. The internal resistance at 10 kHz (real Z' axis) for composites based on SWCNTs, MWCNTs and ox-CNOs were very similar and close to 400 Ω. For the pure C_{60}-Pd polymer the internal resistance is 416 Ω. In Fig. 13, the relation between the real and imaginary capacitance as a function of frequency is shown. From the $C'' - \log f$ relation, a relatively small value of the relaxation time τ_o was observed (Fig. 13a), indicating that the system passes the frontier between resistive and capacitive

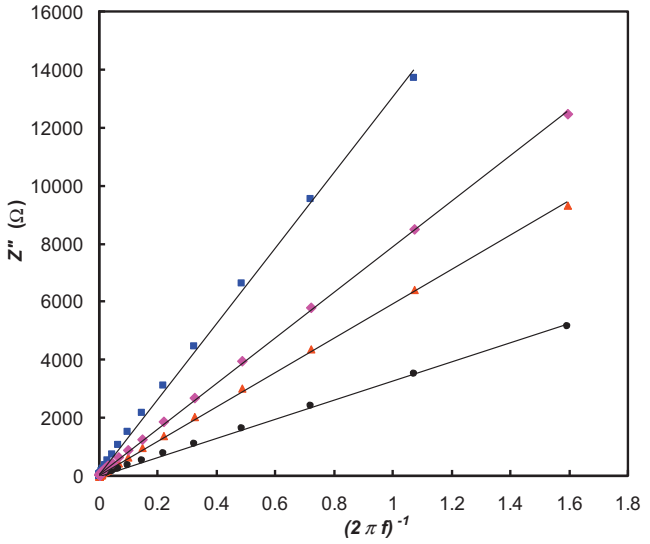

Fig. 14. Dependence of the imaginary part of impedance on reciprocal of the frequency for (♦) C_{60}-Pd polymer, (●) SWCNTs/C_{60}-Pd, (▲) MWCNTs/C_{60}-Pd and (■) ox-CNOs/C_{60}-Pd films in acetonitrile containing 0.10 M (TBA)ClO_4 at -1200 mV. The composites containing (●) 3.90 μg SWCNTs and 0.77 μg C_{60}-Pd, (▲) 3.93 μg MWCNTs and 0.68 μg C_{60}-Pd and (■) 3.36 μg ox-CNOs and 0.65 μg C_{60}-Pd. The mass of the C_{60}-Pd polymer deposited at the bare gold electrode was 0.531 μg. (For interpretation of the references to color in this figure legend, the reader is referred to the web version of this article.)

behavior very quickly. The smallest value of the relaxation time was obtained for the ox-CNOs/C_{60}-Pd. The values of capacitance were calculated according to the equation:

$$C = (2\pi f\, Z'')^{-1} \quad (4)$$

From the slope of the linear correlation between the imaginary impedance and the reciprocal of the frequency (Fig. 14), specific capacitances of 397 F g^{-1}, 249 F g^{-1} and 118 F g^{-1} were obtained for SWCNTs/C_{60}-Pd, MWCNTs/C_{60}-Pd and ox-CNOs/C_{60}-Pd, respectively. For comparison, the specific capacitance obtained for C_{60}-Pd is 239 F g^{-1}. The EIS capacitance values follow the capacitances obtained from cyclic voltammograms. The values of the capacitances obtained from the limiting value of $C' - log\ f$ dependences and from the linear relations between Z'' and the recriprocal of $2\pi f$ are very similar. The values of capacitance, calculated from the C'–$log\ f$ relation are 386 F g^{-1}, 246 F g^{-1} and 115 F g^{-1}, 237 F g^{-1} respectively, for SWCNTs/C_{60}-Pd, MWCNTs/C_{60}-Pd, ox-CNOs/C_{60}-Pd and for the C_{60}-Pd polymer.

4. Conclusions

Composites containing a C_{60}-Pd polymer and different carbon nanostructures, such as SWCNTs, MWCNTs, and ox-CNOs, were prepared by electrochemical polymerization of C_{60}-Pd onto thin films of the carbon nanostructures immobilized on an electrode surface. The materials exhibit porous structures. The most compact film was obtained for the ox-CNO/C_{60}-Pd composite. All materials are electrochemically active at negative potentials due to fullerene moiety reduction. All composites also exhibit good electrochemical stability under multicyclic voltammetric conditions. Both mechanical and electrochemical stabilities increase significantly compared to the pure C_{60}-Pd polymer. The composites also give fast current responses upon potential changes. The lowest relaxation time, equal to 30 ms, which is related to a transition between conducting and non conducting states, was obtained for ox-CNO/C_{60}-Pd. The porous structure of the composites confer also good capacitance properties. Limiting values of 994, 758, and 284 F g^{-1} were found for SWCNTs/C_{60}-Pd, MWCNTs/C_{60}-Pd and ox-CNOs/C_{60}-Pd, respectively. These values are much higher compared to the specific capacitance of the pure C_{60}-Pd polymer. Therefore the composites are very promising materials for the preparation of supercapacitors.

Acknowledgements

The authors acknowledge the National Center of Science (project No. 2011/01/B/ST5/0627 to KW) for a financial support. L.E. thanks the Robert A. Welch Foundation for an endowed chair, grant #AH-0033 and the US NSF, grant CHE-1110967. TEM and SEM was funded by ERDF, as part of the Operational Programme Development of Eastern Poland 2007–2013, project Nr POPW.01.03.00-20-034/09-00.

References

[1] O. Barberi, M. Hahn, A. Herzog, R. Kotz, Capacitance limits of high surface area activated carbons for double layer capacitors, Carbon 43 (2005) 1303.
[2] R. Salinger, U. Fischer, C. Herta, J. Fricke, High surface area carbon aerogels for supercapacitors, Journal of Non-Crystalline Solids 225 (1998) 81.
[3] J.A. Fernandez, S. Tennison, O. Kozynchenko, F. Rubiera, F. Stoeckli, T.A. Centeno, Effect of mesoporosity on specific capacitance of carbons, Carbon 47 (2009) 1598.
[4] A.B. Fuertes, F. Pico, J.M. Rojo, Influence of pore structure on electric double-layer capacitance of template mesoporous carbons, Journal of Power Sources 133 (2004) 329.
[5] X.Y. Tao, X.B. Zhang, L. Zhang, J.P. Cheng, F. Liu, J.H. Luo, Z.Q. Luo, H.J. Geise, Synthesis of multi-branched porous carbon nanofibers and their application in electrochemical double-layer capacitors, Carbon 44 (2004) 1425.
[6] M. Arylepp, J. Leis, M. Latt, F. Miller, K. Rumma, E. Lust, A.F. Burke, Preparation of carbon aerogel electrodes for supercapacitor and their electrochemical characteristics, Journal of Power Sources 162 (2006) 1460.
[7] S.J. Kim, S.W. Hwang, S.H. Hyun, Preparation of carbon aerogel electrodes for supercapacitor and their electrochemical characteristics, Journal of Materials Science 40 (2005) 725.
[8] E. Frackowiak, Carbon materials for supercapacitor application, Physical Chemistry Chemical Physics 9 (2007) 1774.
[9] W. Xing, S.Z. Qiao, R.G. Ding, F. Li, G.Q. Lu, Z.F. Yan, H.M. Cheng, Superior electric double layer capacitors using ordered mesoporous carbon, Carbon 44 (2006) 216.
[10] G. Yuan, Z. Jiang, A. Aramata, Y. Gao, Electrochemical behavior of activated-carbon capacitor material loaded with nickel oxide, Carbon 43 (2005) 2913.
[11] H. Jiang, J. Ma, Ch. Li, Mesoporous carbon incorporated metal oxide nanomaterials as supercapacitor electrodes, Advanced Materials 24 (2012) 4197.
[12] J.M. Ko, K.S. Ryu, S. Kim, K.M. Kim, Supercapacitive properties of composite electrodes consisting of polyaniline, carbon nanotube, and RuO_2, Journal of Applied Electrochemistry 39 (2009) 1331.
[13] E. Raymundo-Piñero, V. Khomenko, E. Frackowiak, F. Béguin, Performance of manganese oxide/CNTs composite as electrode materials for electrochemical capacitors, Journal of Electrochemical Society 152 (2005) A229.
[14] M. Ramani, B.S. Haran, R.E. White, B.N. Popov, L. Arsov, Studies on activated carbon capacitor materials loaded with different amounts of ruthenium oxide, Journal of Power Sources 93 (2001) 209.
[15] K. Jurewicz, S. Delpeux, V. Bertagna, F. Béguin, Supercapacitors from nanotubes/polypyrrole composites, Chemical Physics Letters 347 (2001) 36.
[16] E. Frackowiak, V. Khomenko, K. Jurewicz, K. Lota, F. Béguin, Supercapacitors based on conducting polymers/nanotubes composites, Journal of Power Sources 153 (2006) 413.
[17] M.J. Bleda-Martínez, Ch. Peng, S. Zhang, G.Z. Chen, E. Morallón, D. Cazorla-Amorós, Electrochemical methods to enhance the capacitance in activated carbon/polyaniline composites, Journal of Electrochemical Society 155 (2008) A672.
[18] M. Oh, S. Kim, Preparation and electrochemical characterization of polyaniline/activated carbon composites as an electrode material for supercapacitors, Journal of Nanoscience and Nanotechnology 12 (2012) 519.
[19] W. Chen, Z. Fan, L. Gu, X. Bao, Ch. Wang, Enhanced capacitance of manganese oxide via confinement inside carbon nanotubes, Chemical Communications 46 (2010) 3905.
[20] S. Iijima, Helical microtubules of graphitic carbon, Nature 354 (1991) 56.
[21] V.V. Abalyaeva, N.N. Vershinin, Yu.M. Shul'ga, O.N. Efimov, The composites of polyaniline with multiwall carbon nanotubes: preparation, electrochemical properties, and conductivity, Russian Journal of Electrochemistry 45 (2009) 1266.
[22] V. Brânzoi, F. Brânzoi, L. Pilan, N. Donisan, The characterization of some nanocomposites based on conducting polymers and carbon nanotubes obtained by co-polymerization, Roumania Journal of Chemistry 55 (2010) 369.
[23] G.A. Snook, P. Kao, A.S. Best, Conducting-polymer-based supercapacitor devices and electrodes, Journal of Power Sources 196 (2011) 1.
[24] G. Lota, K. Fic, E. Frackowiak, Carbon nanotubes and their composites in electrochemical applications, Energy & Enviromental Science 4 (2011) 1592.

[25] Y. Xu, S.-Q. Zhuang, X.-Y. Zhang, P.-G. He, Y.-Z. Fang, Configuration and capacitance properties of polypyrrole/aligned carbon nanotubes synthesized by electropolymerization, Chinese Science Bulletin 56 (2011) 3823.
[26] A. Bahrami, Z.A. Talib, E. Shahriari, W.M.M. Yunus, A. Kasim, K. Behzad, Characterization of electrosynthesized conjugated polymer-carbon nanotube composite: optical nonlinearity and electrical property, International Journal of Molecular Sciences 13 (2012) 918.
[27] B. Zhang, Y. Xu, Y. Zheng, L. Dai, M. Zhang, J. Yang, Y. Chen, X. Chen, J. Zhou, A facile synthesis of polypyrrole/carbon nanotube composites with ultrathin, uniform and thickness-tunable polypyrrole shells, Nanoscale Research Letters 6 (2011) 431.
[28] J. Wang, C.O. Too, D. Zhou, G.G. Wallace, Novel electrode substrates for rechargeable lithium/polypyrrole batteries, Journal of Power Sources 140 (2005) 162.
[29] S.R. Sivakkumar, J.-S. Oh, D.-W. Kim, Polyaniline nanofibres as a cathode material for rechargeable lithium-polymer cells assembled with gel polymer electrolyte, Journal of Power Sources 163 (2006) 573.
[30] Y. Zhou, Z.-Y. Qin, L. Li, Y. Zhang, Y.-L. Wei, L.-F. Wang, M.-F. Zhu, Polyaniline/multi-walled carbon nanotube composite with core-shell structures as supercapacitor electrode materials, Electrochimica Acta 55 (2010) 3904.
[31] J. Chen, Y. Liu, A.I. Minett, C. Lynam, J. Wang, G.G. Wallace, Flexible, aligned carbon nanotube/conducting polymer electrodes for a lithium-ion battery, Chemistry of Materials 19 (2007) 3595.
[32] S.R. Sivakkumar, W.J. Kim, J. -A. Choi, D.R. MacFarlane, M. Forsyth, D. -W. Kim, Electrochemical perfomance of polyaniline nanofibres and polyaniline/multi-walled carbon nanotube composite as an electrode material for aqueous redox supercapacitors, Journal of Power Sources 171 (2007) 1062.
[33] E. Zawadzka, R. Kukliński, B. Szubzda, B. Mazurek, Polyaniline – multi-walled carbon nanotube shell-core composite as an electrode material in supercapacitors, Materials Science (Poland) 27 (2009) 1271.
[34] Ch. Peng, S. Zhang, D. Jewell, G.Z. Chen, Carbon nanotube and conducting polymer composites for supercapacitors, Progress in Natural Science 18 (2008) 777.
[35] B. Dong, B.-L. He, C.-L. Xu, H.-L. Li, Preparation and electrochemical characterization of polyaniline/multi-walled carbon nanotubes composites for supercapacitor, Materials Science and Engineering 143 (2007) 7.
[36] S. Paul, Y.-S. Lee, J.-A. Choi, Y.Ch. Kang, D.-W. Kim, Synthesis and electrochemical characterization of polypyrrole/multi-walled carbon nanotube composite electrodes for supercapacitor applications, Bulletin of the Korean Chemical Society 31 (2010) 1228.
[37] J. Wang, M. Musameh, Carbon-nanotubes doped polypyrrole glucose biosensor, Analytica Chimica Acta 539 (2005) 209.
[38] X. Luo, A.J. Killard, A. Morrin, M.R. Smyth, Ehancement of a conducting polymer-based biosensor using carbon nanotube-doped polyaniline, Analytica Chimica Acta 575 (2006) 39.
[39] R.B. Rakhi, K. Sethupathi, S. Ramaprabhu, Electron field emission properties of conducting polymer coated multi walled carbon nanotubes, Applied Surface Science 254 (2008) 6770.
[40] Y.W. Jin, J.E. Jung, Y.J. Park, J.H. Choi, D.S. Jung, H.W. Lee, S.H. Park, N.S. Lee, J.M. Kim, T.Y. Ko, S.J. Lee, S.Y. Hwang, J.H. You, J.-B. Yoo, Ch.-Y. Park, Triode-type field emission array using carbon nanotubes and a conducting polymer composite prepared by electrochemical polymerization, Journal of Applied Physics 92 (2002) 1065.
[41] P. Hojati-Talemi, G.P. Simon, Electropolymerization of polypyrrole/carbon nanotube composite films over an electrically nonconductive membrane, Journal of Physical Chemistry C 114 (2010) 13962.
[42] E. Frackowiak, F. Béguin, Electrochemical storage of energy in carbon nanotubes and nanostructured carbons, Carbon 40 (2002) 1775.
[43] X.L. Chen, W.S. Li, C.L. Tan, W. Li, Y.Z. Wu, Improvement in electrochemical capacitance of carbon materials by nitric acid treatment, Journal of Power Sources 184 (2008) 668.
[44] J.H. Chen, W.Z. Li, D.Z. Wang, S.X. Yang, J.G. Wen, Z.F. Ren, Electrochemical characterization of carbon nanotubes as electrode in electrochemical double-layer capacitors, Carbon 40 (2002) 1193.
[45] E. Frackowiak, F. Béguin, Carbon materials for the electrochemical storage of energy in capacitors, Carbon 39 (2001) 937.
[46] E. Frackowiak, K. Metenier, V. Bertagna, F. Béguin, Supercapacitor electrodes from multiwalled carbon nanotubes, Applied Physics Letters 77 (2000) 2421.
[47] Q. Xiao, X. Zhou, The study of multiwalled carbon nanotube deposited with conducting polymer for supercapacitor, Electrochimica Acta 48 (2003) 575.
[48] J. Zhang, L.-B. Kong, B. Wang, Y.-Ch. Luo, L. Kang, In-situ electrochemical polymerization of multi-walled carbon nanotube/polyaniline composite films for electrochemical supercapacitors, Synthetic Metals 159 (2009) 260.
[49] M. Wu, G.A. Snook, V. Gupta, M. Shaffer, D.F. Fray, G.Z. Chen, Electrochemical fabrication and capacitance of composite films of carbon nanotubes and polyaniline, Journal of Materials Chemistry 15 (2005) 2297.
[50] Ch. Peng, J. Jin, G.Z. Chen, A comparative study on electrochemical co-deposition and capacitance of composite films of conducting polymers and carbon nanotubes, Electrochimica Acta 53 (2007) 525.
[51] V. Khomenko, E. Frackowiak, F. Béguin, Determination of the specific capacitance of conducting polymer/nanotubes composite electrodes using different cell configurations, Electrochimica Acta 50 (2005) 2499.
[52] S.C. Canobre, D.A.L. Almeida, C.P. Fonesca, S. Neves, Synthesis and characterization of hybrid composites based on carbon nanotubes, Electrochimica Acta 54 (2009) 6383.
[53] W. Xing, S. Zhuo, H. Cui, W. Si, X. Gao, Z. Yan, Enhanced electrochemical properties of polyaniline-coated multiwall carbon nanotubes, Journal of Porous Materials 15 (2008) 647.
[54] Y. Zhou, Z.-Y. Qin, L. Li, Y. Zhang, Y.-L. Wei, L.-F. Wang, M.-F. Zhu, Polyaniline/multi-walled carbon nanotube composites with core-shell structures as supercapacitor electrode materials, Electrochimica Acta 55 (2010) 3904.
[55] M. Hughes, G.Z. Chen, M.S.P. Shaffer, D.J. Fray, A.H. Windle, Electrochemical capacitance of a nanoporous composite of carbon nanotubes and polypyrrole, Chemistry of Materials 14 (2002) 1610.
[56] J. Wang, Y. Xu, X. Chen, X. Sun, Capacitance properties of single wall carbon nanotube/polypyrrole composite films, Composites Science and Technology 67 (2007) 2981.
[57] Y. Zhou, B. He, W. Zhou, J. Huang, X. Li, B. Wu, H. Li, Electrochemical capacitance of well-coated single-walled carbon nanotube with polyaniline composites, Electrochimica Acta 49 (2004) 257.
[58] K. Lota, V. Khomenko, E. Frackowiak, Capacitance properties of poly(3,4-ethylenedioxythiophene)/carbon nanotubes composites, Journal of Physics and Chemistry of Solids 65 (2004) 295.
[59] V. Gupta, N. Miura, Influence of the microstructure on the supercapacitive behavior of polyaniline/single-wall carbon nanotube composites, Journal of Power Sources 157 (2006) 616.
[60] P. Gajendran, R. Saraswathi, Polyaniline-carbon nanotube composites, Pure and Applied Chemistry 80 (2008) 2377.
[61] Ch. Zhou, S. Kumar, C.D. Doyle, J.M. Tour, Functionalized single wall carbon nanotubes treated with pyrrole for electrochemical supercapacitor membranes, Chemistry of Materials 17 (2005) 1997.
[62] E. Frackowiak, K. Jurewicz, S. Delpeux, F. Béguin, Nanotubular materials for supercapacitors, Journal of Power Sources 97–98 (2001) 822.
[63] J.N. Barsici, G.G. Wallace, R.H. Baughman, Electrochemical studies of single-wall carbon nanotubes in aqueous solutions, Journal of Electroanalytical Chemistry 488 (2000) 92.
[64] A.G. Krivenko, V.I. Matyushenko, E.V. Stenina, L.N. Sviridova, A.V. Krestinin, G.I. Zvereva, V.A. Kurmaz, A.G. Ryabenko, S.N. Dmitriev, V.A. Skuratov, Peculiarities of the electrochemical behavior of modified electrodes containing single-wall carbon nanotubes, Electrochemistry Communications 7 (2005) 199.
[65] G. Arable, D. Wagh, M. Kulkarni, I.S. Mulla, S.P. Vernekar, K. Vijayamohanan, A.M. Rao, Enhanced supercapacitance of multiwalled carbon nanotubes functionalized with ruthenium oxide, Chemical Physics Letters 376 (2003) 207.
[66] J. Oh, M.E. Kozlov, B.G. Kim, H.-K. Kim, R.H. Baughman, Y.H. Hwang, Preparation and electrochemical characterization of porous SWNT-PPy nanocomposite sheets for supercapacitor applications, Synthetic Metals 158 (2008) 638.
[67] A. Palkar, F. Melin, C.M. Cardona, B. Elliott, A.K. Naskar, D.D. Edie, A. Kumbhar, L. Echegoyen, Reactivity differences between carbon nano onions (CNOs) prepared by different methods, Chemistry: An Asian Journal 2 (2007) 625.
[68] M.E. Plonska-Brzezinska, A. Palkar, K. Winkler, L. Echegoyen, Electrochemical properties of small carbon nano-onion films, Electrochemical and Solid State Letters 13 (2010) K35.
[69] E. Grodzka, P. Pieta, P. Dłużewski, W. Kutner, K. Winkler, Formation and electrochemical properties of composites of the C_{60}-Pd polymer and multi-wall carbon nanotubes, Electrochimica Acta 54 (2009) 5621.
[70] K. Winkler, K. Noworyta, W. Kutner, A.L. Balch, Study of redox active C_{60}/Pd films by simultaneous cyclic voltammetry and piezoelectric microgravimetry at an electrochemical quartz crystal microbalance, Journal of Electrochemical Society 147 (2000) 2597.
[71] A.L. Balch, D.A. Costa, K. Winkler, Formation of redox-active, two-component films by electrochemical reduction of C_{60} and transition metal complexes, Journal of the American Chemical Society 120 (1998) 9614.
[72] K. Winkler, A. de Bettecourt-Dias, A.L. Balch, Charging processes in electroactive C_{60}/Pd films: effect of solvent and supporting electrolyte, Chemistry of Materials 11 (1999) 2265.
[73] K. Winkler, A. de Bettencourt-Dias, A.L. Balch, Electrochemical studies of C_{60}/Pd films formed by the reduction of C_{60} in the presence of palladium (II) acetate trimer. Effects of varying C_{60}/Pd (II) ratios in the precursor solutions, Chemistry of Materials 12 (2000) 1386.
[74] K. Winkler, K. Noworyta, A. de Bettecourt-Dias, J.W. Sobczak, Ch.-T. Wu, L.-Ch. Chen, W. Kutner, A.L. Balch, Structure and properties of C_{60}-Pd films formed by electroreduction of C_{60} and palladium (II) acetate trimer: evidence for the presence of palladium nanoparticles, Journal of Materials Chemistry 13 (2003) 518.
[75] K. Winkler, A.L. Balch, Electrochemically formed two-component films comprised of fullerene and transition-metal components, Comptes Rendus Chimie 9 (2006) 928.
[76] H. Nagashima, A. Nakaoka, Y. Saito, M. Kato, T. Kawanishi, K. Itoh, $C_{60}Pd_n$: the first organometallic polymer of buckminsterfullerene, Journal of the Chemical Society, Chemical Communications (1992) 377.
[77] K. Winkler, A.L. Balch, W. Kutner, Electrochemically formed fullerene-based polymeric films, Journal of Solid State Electrochemistry 10 (2006) 761.
[78] K. Winkler, E. Grodzka, F. D'Souza, A.L. Balch, Two-component films of fullerene and palladium as materials for electrochemical capacitors, Journal of The Electrochemical Society 154 (2007) K1.
[79] E. Grodzka, J. Grabowska, M. Wysocka-Żołopa, K. Winkler, Electrochemical formation and properties of two-component films of transition metal complexes and C_{60} or C_{70}, Journal of Solid State Electrochemistry 12 (2008) 1267.
[80] E. Brancewicz, E. Grądzka, K. Winkler, Comparison of electrochemical properties of two-component C_{60}-Pd polymers formed under electrochemical

conditions and by chemical synthesis, Journal of Solid State Electrochemistry (2013), http://dx.doi.org/10.1007/s10008-012-1982-2.
[81] P. Pieta, E. Grodzka, K. Winkler, M. Warczak, A. Sadkowski, G.Z. Zukowska, G.M. Venukadasula, F. D'Souza, W. Kutner, Conductive, capacitive, and viscoelastic properties of a new composite of the C_{60}-Pd conducting polymer and single-wall carbon nanotubes, Journal of Physical Chemistry B 113 (2009) 6682.
[82] P. Pieta, E. Grodzka, K. Winkler, G.M. Venukadasula, F. D'Souza, W. Kutner, Preparation and selected properties of a composite of the C_{60}-Pd conducting polymer and single-wall carbon nanotubes, Physica Status Solidi B 245 (2008) 2292.
[83] D. Suppiger, S. Busato, P. Ermanni, M. Motta, A. Windle, Electrochemical actuation of macroscopic carbon nanotube structures: mats and aligned ribbons, Physical Chemistry Chemical Physics 11 (2009) 5180.
[84] S.R.C. Vivekchand, C.S. Rout, K.S. Subrahmanyam, A. Govindaraj, C.N.R. Rao, Graphene-based electrochemical supercapacitors, Journal of Chemical Sciences 120 (2008) 9.
[85] S. Bose, T. Kuila, A.K. Mishra, R. Rajasekar, N.H. Kim, J.H. Lee, Carbon-based nanostructured materials and their composites as supercapacitor electrodes, Journal of Materials Chemistry 22 (2012) 767.
[86] S. Amokrane, J.P. Badiali, A new analysis of the differential capacitance of an ideally polarized electrode, Journal of Electroanalytical Chemistry 266 (1989) 21.
[87] J.P. Badiali, The jellium model in electrochemistry, Berichte der Bunsengesellschaft für physikalische Chemie 91 (1987) 270.
[88] S. Amokrane, J.P. Badiali, A new analysis of the differential capacitance of an ideally polarized electrode: Part II. Non-aqueous solvents, Journal of Electroanalytical Chemistry 297 (1991) 377.
[89] J. Sobkowski, Interaction of solvents with metallic surfaces, Polish Journal of Chemistry 67 (1993) 773.
[90] E. Grodzka, M. Nieciecka, K. Winkler, Stability studies of an electrochemically formed [C_{60}] fullerene-palladium two-component film, Journal of Solid State Electrochemistry 12 (2008) 215.